LA-UR-17-25199 (Accepted Manuscript)

# Low hygroscopicity of ambient fresh carbonaceous aerosols from pyrotechnics smoke

Dubey, Manvendra Krishna
Carrico, Christian
Bixler, Samantha Laray
Aiken, Allison C.



**To be published in:** Atmospheric Environment

**DOI to publisher's version:** 10.1016/j.atmosenv.2018.01.024

**Permalink to record:** http://permalink.lanl.gov/object/view?what=info:lanl-repo/lareport/LA-UR-17-25199

# Accepted Manuscript

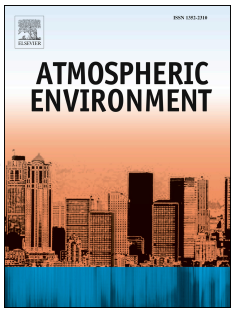


Low hygroscopicity of ambient fresh carbonaceous aerosols from pyrotechnics smoke

Christian M. Carrico, Samantha L. Bixler, Manvendra K. Dubey, Allison C. Aiken

PII: S1352-2310(18)30038-4

DOI: 10.1016/j.atmosenv.2018.01.024

Reference: AEA 15783

To appear in: *Atmospheric Environment*

Received Date: 27 June 2017

Revised Date: 28 December 2017

Accepted Date: 13 January 2018

Please cite this article as: Carrico, C.M., Bixler, S.L., Dubey, M.K., Aiken, A.C., Low hygroscopicity of ambient fresh carbonaceous aerosols from pyrotechnics smoke, *Atmospheric Environment* (2018), doi: 10.1016/j.atmosenv.2018.01.024.

Re-submission to Atmospheric Environment

# Low Hygroscopicity of Ambient Fresh Carbonaceous Aerosols from Pyrotechnics Smoke

**Christian M. Carrico*, Samantha L. Bixler** New Mexico Institute of Mining and Technology, Socorro, NM 87801

**Manvendra K. Dubey, Allison C. Aiken** Los Alamos National Laboratory, Los Alamos, NM 87545

## HIGHLIGHTS

1. Pyrotechnics (fireworks) have substantial though episodic impacts on ambient aerosol properties.
2. In a well-mixed < 3 hr old fireworks plume, dry light scattering (450 nm) reached 120 $Mm^{-1}$ with nearly constant ω (780nm) = 0.86 and Å = 2.2.
3. Ambient fireworks smoke aerosol hygroscopic response was low ($f$(RH=85%) ~ 1), implying lower radiative effects but longer lifetime and potential human exposures.
4. Chemical composition was a key driver as smoke from small sparklers exhibited greater water uptake (due to the contribution of potassium chloride) than from the larger explosive aerial fireworks which were likely dominated by organic and elemental carbon.

* Correspondence to: C.M. Carrico, kip.carrico@nmt.edu

# ABSTRACT

Pyrotechnics (fireworks) displays are common for many cultures worldwide, with Independence Day celebrations occurring annually on July 4$^{th}$ as the most notable in the U.S. Given an episodic nature, fireworks aerosol properties are poorly characterized. Here we report observations of optical properties of fresh smoke emissions from Independence Day fireworks smoke sampled at Los Alamos National Laboratory, New Mexico U.S.A. on 4-5 July 2016. Aerosol optical properties were measured with a photoacoustic extinctiometer (PAX, DMT, Inc., Model 870nm) at low RH < 30% and a humidity controlled nephelometry system (Ecotech, Inc., 450 nm Aurora). 'Dry' light scattering coefficient ($\sigma_{sp}$) increased from background < 15 $Mm^{-1}$ reaching 120 $Mm^{-1}$ (450 nm) as a 2-minute event peak, while the absorption coefficient increased from background of 0.5 to 4.4 $Mm^{-1}$ (870 nm). The event peak occurred at 00:35 on 5 July 2016, ~3 hours after local fireworks events, and decreased to background by 04:00 on 5 July 2016, showing well mixed aerosol properties. A notable result is that the aerosol hygroscopic response, as characterized by the ratio of wet to dry light scattering or *f*(RH=85%), declined to 1.02 at the peak fireworks influence from a background ~1.7. Strong wavelength dependence of light scattering with Ångström exponent ~ 2.2 throughout the event showed a size distribution dominated by sub-micrometer particles. Likewise, single scattering albedo at 870 nm remained constant throughout the event with $\omega = 0.86 \pm 0.03$, indicating light absorbing carbon, though not dominant, was mixed with organic carbon. Subsequent laboratory testing with ground-level sparklers showed that pyrotechnics smoke can generate a strong hygroscopic response, however. As confirmed with chemical analysis, the chemistry of the fireworks was key to defining the hygroscopic response. Sparkler smoke was dominated by salt species such as hygroscopic potassium chloride while it lacked the black powder explosives in aerial fireworks that contribute organic and elemental carbon to its non-hygroscopic smoke.

# 1 INTRODUCTION

## 1.1 Particulate Material ($PM_{2.5}$) and Its Air Quality Impacts

Particulate material, particularly the fine fraction (i.e. small particles < 2.5 µm diameter), has important impacts on atmospheric chemistry and optics. Particulate matter with aerodynamic diameters less than 2.5 micrometers ($PM_{2.5}$) is a specific parameter of interest to human health, atmospheric visibility, and climate. $PM_{2.5}$ has primary and secondary sources it is responsible for substantial atmospheric light extinction, penetrates deeply into the human lungs, and is a source of cloud condensation nuclei. Traditionally in the U.S., the regulatory focus has been on $PM_{2.5}$ as the basis for human health impacts [*Pope and Dockery*, 2006]. Recently, interest has also developed in $D_p$ < 1 µm ($PM_1$) and ultrafine particles ($D_p$ < 100 nm) which often dominate number concentrations freshly emitted from combustion sources [*Carrico et al.*, 2016a]; the European Union currently has regulatory statutes addressing ultrafine particles. The sources of these particles are diverse and include many anthropogenic contributions, largely from combustion sources, as well as from new particle formation from natural and anthropogenic precursors. Here we examine the microphysical properties of 2-3 hours old smoke from the combustion of pyrotechnics (fireworks) associated with the U.S. Independence Day celebration in 2016.

## 1.2 Fireworks Emissions and Air Quality

Fireworks displays are common globally across many cultures, associated with select secular and religious events. Emissions from fireworks represent a distinct though transient impact on local to regional air quality. In the U.S., the most important fireworks event is Independence Day on July 4$^{th}$, with 75% of professional and 90% of retail fireworks sales associated with the event according to the American Pyrotechnics Association (APA). Moreover, fireworks sales have increased from 41 to 285 million pounds of fireworks from 1980 to 2015 in the U.S. alone (APA data). In 2015, revenues from consumer sales were $0.76 billion vs. $0.34 billion for display fireworks (APA data). Thus, the emissions in the U.S. are distributed beyond major professional displays and likely track population density among other factors. Differences are expected as a function of height, as consumer fireworks are closer to ground level vs. those in professional displays.

Gas-phase and particle emissions from fireworks may differ substantially from those from fuels combustion. For example, ozone formation can be impacted by fireworks, as they can serve as a direct formation mechanism for ozone in addition to emission of precursors [*Attri et al.*, 2001]. Some studies have shown some elevated $NO_x$ while other studies have shown negligible impacts on $NO_x$ and ozone [*Mandal et al.*, 2012; *Parkhi et al.*, 2016]. Due to its oxidative capacity fireworks smoke has been implicated as a health risk for acute cardio-respiratory effects [*Godri et al.*, 2010].

### 1.3 Particulate Material Properties from Fireworks Smoke

Nearly universally, observations show elevated PM and particularly ultrafine and accumulation mode particles associated with emissions from fireworks. They are a substantial though short-lived source of fine mode particulate material ($PM_{2.5}$) including trace metal species [*Drewnick et al.*, 2006; *Moreno et al.*, 2007]. One of the most comprehensive fireworks-related studies examined a network of 315 U.S. ambient aerosol monitoring stations over multiple years [*Seidel and Birnbaum*, 2015]. Observations showed recurrent, though short-lived (<0.5 days), impacts associated with U.S. Independence Day fireworks at urban U.S. monitoring stations [*Seidel and Birnbaum*, 2015]. For example, the study found average hourly $PM_{2.5}$ concentrations elevated by 21 $\mu g/m^3$ during the hour from 19:00-20:00, with a 42% average increase in 24-hour $PM_{2.5}$ concentrations compared to proximate days.

The chemical composition of fireworks is relevant for the resulting smoke properties. The primary composition of fireworks' black powder charge is graphitic carbon, potassium nitrate, and elemental sulfur in varying proportions [*Russell*, 2000]. The black powder is use as a propellant and explosive charge for aerial fireworks, and the products of combustion include potassium compounds [*Russell*, 2000]. There are various emitter compounds, mainly metals, including iron oxides, aluminum, titanium and potassium compounds for coloration. For example, the primary colorants for yellow coloration are sodium salts [*Russell*, 2000]. Nonetheless, organic carbon (OC) species are often the dominant chemical contributor in ambient fireworks observations [*Jiang et al.*, 2015; *Tsai et al.*, 2012].

### 1.4 Southeast Asia Studies of Fireworks Emission Characteristics

The origin of fireworks traces to East Asia, and the Asian continent has a long history in religious and secular festivals [*Russell*, 2000]. Numerous recent studies have examined the significance of fireworks to air quality in south and East Asia, and most notably India, Taiwan, and China [*Chen et al.*, 2016]. Several studies have examined fireworks in India particularly as related to the annual Diwali Festival [*Kumar et al.*, 2016; *Nasir and Brahmaiah*, 2015]. One of the worst smog events in India occurred in New Delhi, India in early November 2016 with $PM_{2.5}$ concentrations exceeding the instrument upper limit of 999 $\mu g/m^3$. It is still under investigation, but it was estimated that 60-70% contributions from fireworks smoke (https://phys.org/news/2016-10-delhi-toxic-smog-diwali-festival.html). As a result, the Supreme Court of India banned the sale of fireworks in 2017, though the air quality impacts were still very significant during the Diwali festival of 2017 (https://phys.org/news/2017-10-delhi-toxic-haze-diwali-fireworks.html).

### 1.5 Optical Properties of Fireworks Aerosols

Many of the measurements of fireworks smoke impacted aerosols have focused on $PM_{2.5}$ mass concentrations and chemical speciation. However, a small number of studies investigated aerosol optical properties of fireworks smoke. The general observations are a fine mode dominance of PM properties and elevated single scattering albedo ($\omega$, the ratio of light scattering to extinction) during impacted time periods [*Devara et al.*, 2015]. In part due to their transitory impacts, data in the literature is lacking on the extent, duration, and characteristics—particularly optical properties—of emissions from fireworks. The intent of this study is to report observations of freshly emitted fireworks generated smoke including optical properties, and in particular, aerosol hygroscopic response as related to the U.S. Independence Day fireworks on 4-5 July 2016.

## 2 EXPERIMENTAL DETAILS

### 2.1 Sampling Site

Measurements were conducted in summer 2016 at Technical Area-51 at Los Alamos National Laboratory (LANL) (Figure 2) located at 35.850˚ N 106.272˚ W at an elevation of 2149 m ASL.

The LANL study was focused on laboratory biomass burning emissions, yet it also provided a unique opportunity to examine ambient fireworks influenced ambient smoke properties. We conducted follow-up laboratory experiments with commercially available sparklers using the same measurement techniques. The following section describes the measurements and experimental quality assurance efforts. *Carrico et al.*, [2016b] gives more details on the experimental methods and results for laboratory combustion of biomass fuels.

The nearest meteorological measurements were ~3 km due north at Los Alamos Municipal Airport (WBAN:93091) which is located at 35.881˚ N 106.276˚ W at an elevation of 2184 m ASL (Figure 2). Local wind direction and speed are reported on a 30-minute average basis and were examined to determine atmospheric transport and source regions. Furthermore, NOAA Hysplit backtrajectory analyses were conducted at the LANL sampling site and the Los Alamos Municipal Airport sites [*Rolph*, 2017; *Stein et al.*, 2015].

Nearby local municipal fireworks displays included White Rock, NM display which was 8.8 km ESE of the LANL sampling site (288 degrees vector from White Rock to LANL site). A public display of fireworks was ignited at Overlook Park in White Rock, NM, for an hour beginning at approximately 21:00 on the evening of 4 July 2016. A public display occurred in Jemez Springs approximately 40 km to the west-southwest of Los Alamos at the same time. Additionally, there were no fewer than six municipal fireworks displays within 200 km of Los Alamos on the evening of 4 July 2016 with unknown contributions including Santa Fe, NM (38 km to the SE), Albuquerque (80 km SSW), Rio Rancho (80 km SSW), Las Vegas (100 km ESE), Grants 163 km WSW), and Farmington (190 km WNW).

### 2.2 Measurement Methods

An aerosol sample inlet extended above roof level of the LANL building at a height of approximately 5-m above ground level. A laminar sample flow of 6 lpm was drawn through a 6.5 mm OD copper tubing, and the aerosol instruments sampled the flow undiluted. Due to the length and pressure drop through the ambient inlet line, no further sample conditioning or size cut was introduced before measurement instrumentation. Combustion sources, particularly with flaming combustion, produce size distributions shifted toward smaller ($D_p$ ~ 50 nm) more

absorbing particles whereas smoldering fires produce larger though still predominantly sub-µm particles ($D_p$ ~ 200 nm) with high ω [*Carrico et al.*, 2016a]. As discussed later, measured wavelength dependence of light scattering (as demonstrated by the unitless Ångström exponent, Å) shows sub-µm mode particles dominated fireworks smoke optical properties. All laboratory smoke measurements were sampled at near ambient conditions undiluted into the instruments, at relative humidity (RH), dry bulb temperature and pressure given in Table 1.

### 2.3 Particle Light Scattering as a Function of Relative Humidity

Relative humidity is an important parameter as it will affect particle water uptake; smoke with a substantial inorganic component is hygroscopic [*Carrico et al.*, 2016b]. Numerous systems for measurement of RH controlled light scattering have been used in past aerosol studies. The instrument described here is based on a simplified version of that described in *Carrico et al.*, [2003] (Figure 1).

The instrument consisted of two integrating nephelometers (Ecotech, Inc., Aurora 450 nm) plumbed in series to measure light scattering coefficients by particles ($\sigma_{sp}$, given in units of inverse length, here 1/Megameters). For our purposes, sampling conditions here (RH < 40%) are considered 'dry,' as hygroscopic diameter growth factors were found to be < 1.02, the instrument uncertainty, for such low humidity [*Carrico et al.*, 2010]. Drying before the dry nephelometer used a membrane drier (Permapure, Inc.) with a dry purge flow, and typically resulted in RH < 20% (Table 1). Humidification of the wet nephelometer used a custom in-line humidifier consisting of a water jacket separated from the aerosol sample flow by a water vapor permeable membrane. During the sampling period discussed here, controlled 'wet' RH = 85.4 +/- 0.6% (arithmetic mean and standard deviation) for the wet nephelometer based on dew point temperature from the upstream Vaisala and the dry bulb temperature measured internal to the nephelometer (Table 1). For both wet and dry instruments, nephelometer inlet temperature and humidity were monitored with a capacitive type sensor (Vaisala Inc., HMT333) interfaced to an analog to digital converter card (National Instruments, Inc. NI-USB 6008). RH instruments were calibrated at high and low RH to within 2% of the RH generated by saturated salt solutions, similar to the 2-3% RH accuracy given as the uncertainty by the manufacturer.

Sample residence time was approximately 4 seconds (s) prior to measurement with the wet nephelometer. Pure $CO_2$ and particle free air were used to calibrate the nephelometers before and after these measurements. Flow rates were verified with external flow standard (BIOS International, Inc., DryCal). All plumbing between the sample inlet and instrument were stainless steel fittings (Swagelok, Inc.) and 1 cm OD electrically-conductive tubing to minimize particle loss.

Nephelometer measurements are reported here for 'as-sampled' conditions (near ambient T, P) with no adjustments for temperature, pressure, instrument non-idealities or other environmental conditions (Table 1). The nephelometer, due to angular limitations and other non-idealities, gives a nephelometer measured total scattering coefficient ($\sigma_{sp}$). *Müller et al.* [2011] used nephelometer-measured wavelength dependence consistent from a single nephelometer and as quantified by the Ångström exponent in deriving a correction to yield 'true' light scattering. Since the long wavelength light scattering measurement here with a photoacoustic extinctiometer (PAX) discussed later [*Nakayama et al.*, 2015] has a different geometry with a smaller truncation error correction is not attempted with this data. Here, using the fireworks smoke measured Ångström derived from the nephelometer plus the PAX, this correction would yield only a slight change in $\sigma_{sp}$ of +3% and thus is ignored here.

### 2.4 Photoacoustic Extinctiometer Measurements

We report particle light scattering and absorption coefficients ($\sigma_{sp}$ and $\sigma_{ap}$) at a frequency of 1-min with a photoacoustic extinctiometer (PAX, Model 870 nm, DMT, Inc.), sampling at a flow rate of approximately 1 lpm [*Arnott et al.*, 1999; *Nakayama et al.*, 2015]. The PAX gives an estimate of the aerosol single scattering albedo ($\omega$, unitless 'brightness' of the aerosol), where $\omega = \sigma_{sp} / [\sigma_{sp} + \sigma_{ap}]$. The instrument sampled through a 0.065 m OD electrically-conductive sampling line, approximately 2 m in length (upstream residence time, $\tau < 3$ s) with no further sample conditioning.

The PAX was calibrated by first using a strongly light scattering aerosol, $(NH_4)_2SO_4$ with complex refractive index of $1.52 \pm 0.01 + 0.00i \pm 0.03i$ at 532 nm [*Lang-Yona et al.*, 2009], followed by a strongly absorbing aerosol generated with a kerosene lamp. Calibrations

compared measured light scattering and absorption to directly measured light extinction applying the Beer-Lambert Law to laser intensity attenuation in the optical cavity [*Arnott et al.*, 2000]. The calibration is not sensitive to the optical properties of the calibration material (e.g., size, refractive index) as high concentrations determine extinction directly from attenuation of the laser intensity using the Beer-Lambert Law. Minor uncertainties are introduced when applying the calibrated response to ambient data due to the fixed geometry of the measurement cell and differences in the scattering phase function for different aerosols [*Nakayama et al.*, 2015]. During measurements, the instrument auto-zeroed periodically on a 15-minute basis by switching a HEPA particle filter in-line

# 3 RESULTS

## 3.1 Measurement Quality Control Checks

A comparison of light scattering coefficients as measured by two nephelometers both at low RH gives indication of the agreement at 'dry' conditions as the wet nephelometer here was controlled to low RH = 33.9 ± 1.7% (Figure 3). These ambient measurements were collected shortly after the fireworks event on 8 July 2016. With respect to ambient $PM_{2.5}$, this period was quite clean with $\sigma_{sp}$ ranging from 7 to 14 $Mm^{-1}$. Agreement between instruments at these low ambient concentrations shows a slope of 0.98, intercept of 0.6 $Mm^{-1}$, and an $R^2$ value of 0.98. The strong agreement at low RH and low magnitude light scattering demonstrates acceptable instrument inter-calibration. The agreement also provides evidence of minimal particle loss through the instruments and humidification system.

## 3.2 Meteorological Context of Ambient Measurements

The meteorology during the period of interest was dry (RH < 21%) and mostly clear with some broken cloud cover from Los Alamos airport measurements obtained from the U.S. National Oceanic and Atmospheric Administration (NOAA) Climate Data Center. A wind rose shows the frequency distribution of windspeed and direction blowing from starting 20:35 4 July 2016 – 08:15 5 July 2016 (36 observations, all times here are given in local MDT). The winds during the period of interest were moderate and steady at 4.5 m/s and westerly origins at 265 degrees (Figure 2).

Air mass back-trajectories calculated backwards for 12 hours and arriving at the LANL sampling site (south site) and at the Los Alamos airport (north site) at heights of 500, 750 and 1000 m also indicated strongly westerly flow aloft (Figure 2) [*Rolph*, 2017; *Stein et al.*, 2015]. The westerly nature of the winds suggests little influence from the nearby White Rocks, NM, fireworks display at approximately 8.8 km to the southeast of the sampling site. At 16 km/h winds and a location 40 km upwind (2.5 hours transit time), we argue that the Jemez Springs, NM fireworks influence was a most likely contributor. The peak impacts occurred > 2 h after the end of municipal displays, and the back-trajectories passed over Jemez Springs (Figure 2). Due to complex mountain meteorological flow characteristics and the nature of numerous fireworks from individual use, the direct source cannot be isolated though.

### 3.3 Ambient Fireworks Aerosol: Extensive Properties

Extensive properties of light scattering and absorption coefficients both increased markedly during the fireworks-dominated episode beginning at approximately 23:45 on 4 July 2016 and lasting until 04:00 on 5 July 2016 (Figure 4). We define the time period of the event by when the light scattering coefficient (450 nm) increased and stayed above typical background values of <15 $Mm^{-1}$ shown previously. As shown in the time series in Figure 4, some small perturbations occurred earlier in $\sigma_{sp}$ around 18:20-19:40 on 4 July 2016. Likewise, some continued influence of fireworks smoke is suspected after 04:00 on 5 July 2016. Both periods are excluded as outside the primary event though. Past studies of combustion aerosols demonstrate that optical properties show significant and rapid changes occurring over time frames on the order of 2 h past initial emission, similar to the transport time observed here [*Carrico et al.*, 2016a; *Vakkari et al.*, 2014].

For four hours before the event light scattering was low and relatively stable, $\sigma_{sp}$ = 9.0 ± 0.5 $Mm^{-1}$ (450 nm). A rapid peak with $\sigma_{sp}$ reaching 120 $Mm^{-1}$ (2-min) occurred at about 00:35 on 5 July 2016, subsequently decreasing througout the morning. Light scattering from both instruments and light absoption from the PAX are highly correlated and show simultaneous peaks. The time period for this event is approximately 3 hours later than the large firework events in this area and as observed at many air quality stations in the U.S. [*Seidel and Birnbaum*, 2015].

The relatively large magnitude and slight change in ω shows only a modest increase in black carbon (BC measured in units of $\mu g/m^3$) associated with the organic carbon in fireworks smoke. PAX-estimated BC concentration increased from 0.1 to 0.36 $\mu g/m^3$ by assuming a mass absorption cross-section for of 4.6 $m^2/g$ at 780nm during the episode. Past measurements with an Aerosol Chemical Speciation Monitor (ACSM) showed predominantly organic carbon (OC) as well as potassium, chloride, and sulfate contributions [*Jiang et al.*, 2015]. Several studies have shown secondary organic aerosol (SOA) predominance, higher OC/EC ratios, and small increases in black carbon all suggesting organic carbon is more important than soot carbon in fireworks smoke [*Tsai et al.*, 2012; *Raju et al.*, 2014]. In *Lin et al.*, [2016], a high absorption Å of 1.4 indicated a substantial brown carbon contribution, not unlike biomass smoke also observed in a study in New York, U.S.A. [*Wang et al.*, 2012]. We do not have any direct measurement of aerosol carbonaceous content but suspect organic carbon, and potentially brown carbon as found in past studies, dominated the aerosol chemical composition.

### 3.4 Ambient Fireworks Aerosol: Intensive Properties

Among intensive properties, ω at 780 nm stayed relatively constant at 0.86 ± 0.03 during the episode, slightly higher than before or after the episode (Figure 4, Table 2). Thus the event did not entail a dramatic shift to a strongly light absorbing aerosol dominated by black carbon. From the photoacoustic instrument, the light scattering and absorption were strongly correlated with $R^2$ = 0.93 thus showing little change in their relationship during the fireworks-dominated event indicating well-mixed properties.

The light scattering coefficients of the shorter wavelength nephelometer (450 nm) exceeded the PAX (870 nm) by a factor of ~four. The wavelength dependence of light scattering was strong with Å = 2.2 ± 0.3 during the event, and this was little changed before, during or after the episode indicating the dominance of the sub-micrometer fraction throughout. Using the episode average Å, we adjusted the scattering to a wavelength of 450 nm to compare directly to the nephelometer. Light scattering measurements from the PAX instrument and nephelometer were highly linear during the event ($R^2$ = 0.95) with a slope of 1.12 indicating little variability in the aerosol size distribution and again a well-mixed aerosol (Figure 5). Finally, the variability in the

intensive optical properties as shown in the standard deviation in Table 2, was much lower during the fireworks plume sampling period also indicating a uniform, well mixed aerosol.

Among aerosol intensive properties, the hygroscopic response was single measured parameter that significantly changed through the event. The enhancment in light scattering due to aerosol hygroscopic growth or *f*(RH=85%) dropped from ~1.7 to a minimum approaching approximately 1.02 during the peak of the episode (Figure 4). We observed an anti-correlation between *f*(RH=85%) and $\sigma_{sp}$ during the event with R = -0.85. For *f*(RH=85%), the minimum was 1.02 and the event average = 1.16 ± 0.10, significantly lower than before or after the event (Table 2). Though the low hygroscopicity means less direct visibility and climate impacts, it also has larger implications for aerosol lifetime and exposure.

*Brock et al.* [2016] proposed a single parameter κ-neph fit for *f*(RH) data. Using *Brock et al.* [2016], κ-neph during the event decreased to a minimum of 0.003 with an event average κ-neph = 0.027 ± 0.017 (Table 2). We take the minimum κ-neph oberserved (κ-neph = 0.003) as associated directly with fireworks emissions and κ-neph = 0.12 as that of the background aerosol (similar to the mean value before and after the event and excluding the suspected perturbations due to fireworks shown in Figure 4). We calculated a 2-component mixture κ-neph weighted by their $\sigma_{sp}$ contributions. We apply a 2-component model where background aerosol $\kappa$ is combined with a fireworks $\kappa$ taken as the minimum reached in Figure 4. These component $\kappa$ values are weighted by the dry light scattering coefficients from the respective cases in real time with background $\sigma_{sp}$ = 9 $Mm^{-1}$ and any excess attributed to fireworks. The tight agreement in Figure 6 for the fireworks influenced case indicates a fairly well-mixed and uniform fireworks aerosol as it reached Los Alamos, also indicated by small variability in Å and ω in Figure 4. Using these inputs and a 2-component mixture, calculated κ is shown versus measured κ-neph for the 4-hour fireworks event from 23:45-04:00 (Figure 6) and the preceding 4 days from 1 July-4 July 2016. The plot shows a strong relationship during the fireworks episode and a much more variable Los Alamos typical aerosol. During the fireworks episode the hygroscopic response roughly follows a 2-component mixture of a nearly hydrophobic fireworks aerosol and a modestly hygroscopic background aerosol.

For combustion processes, one of the most important parameters dictating aerosol physical properties is the MCE as measured in numerous biomass burning aerosol studies. A pronounced relationship between the MCE and ω was described across other FLAME-4 experiments with smoldering combustion characterized by low MCE and leading to high ω [*Liu et al.*, 2014] and leading to a shift to larger sizes [*Carrico et al.*, 2016a]. Using *Liu et al.*, [2014] and their relationship of ω to MCE, the fireworks aerosol represented combustion with MCE ~ 0.92 which is the transition between flaming and smoldering.

### 3.5 Laboratory Sparkler Measurements

We followed the ambient observations with a short laboratory experiment generating pyrotechnics smoke using two types of sparklers, "Colored Sparklers" manufactured in China and "Gold Sparklers" manufactured in Thailand purchased at local fireworks vendors in New Mexico, USA. In previous studies, a significant source of smoke at the ground-level is from sparklers, and emissions were dominated by ultrafine particles $D_p$ < 50 nm comprising 83% of number concentrations [*Betha and Balasubramanian*, 2014]. During Diwali festival in India, sparklers were found to be a strong contributor to near ground-level PM spikes [*Yerramsetti et al.*, 2013].

The smoke from both sparkler varieties measured here was strongly hygroscopic (Table 3), in sharp contrast to the ambient-sampled fireworks influenced properties. Sparklers lack the black powder explosive in aerial fireworks but produce their spark coloration from potassium and sodium salts (http://www.compoundchem.com/2014/11/04/sparklers/). Analysis of major ions (ion chromatography) and carbonaceous content (Sunset Laboratories Organic and Elemental Carbon Analyzer) of PM1 from the smoke generated from sparkler combustion confirms the dominance of potassium and chloride for both sparkler samples (Figure 7). The lower response associated with the Gold Sparkler from Thailand relates to its somewhat smaller contribution from potassium chloride and larger contribution from organic and elemental carbon (Figure 7). Numerous ambient studies have linked fireworks smoke with tracers including elevated trace potassium and chloride ions [*Lin et al.*, 2014; *Yao et al.*, 2015; *Kong et al.*, 2015]. Potassium chloride is a strongly hygroscopic salt that is also an important component of biomass smoke [*Carrico et al.*, 2010].

These properties require further study to determine a complete and systematic description of the controlling variables, but we argue that chemical composition plus combustion characteristics of the pyrotechnics will have a profound influence on smoke properties. Due to the composition of sparklers (including colorant compounds such as potassium chloride) vs. aerial fireworks (black powder explosives), sparkler smoke hygroscopicity was found to contrast (dominated by hygroscopic inorganic salts for the former rather than non-hygroscopic carbonaceous material from black powder combustion products for the latter). . As observed with biomass smoke, fireworks smoke aerosol microphysical and chemical properties and fuel composition determine air quality impacts [*Reid et al.*, 2005a; *Reid et al.*, 2005b]. In a congruent way, biomass burning is a key source of particulate organic carbon (OC), elemental carbon (EC), 'brown' carbon that absorbs radiation at shorter wavelengths, [*Bond et al.*, 2013; *Saleh et al.*, 2014] as well as inorganic species that are fuel dependent [*Carrico et al.*, 2016b].

# 4 DISCUSSION AND CONCLUSION

Impacts on air quality from fireworks have been receiving increasing attention, particularly in high population density developing countries like India and China where acute impacts are observed. This is also a concern in the U.S. with potential exposure to fireworks emissions, particularly to sensitive populations. Here we measured aerosol optical properties including aerosol light scattering, its wavelength dependence, light absorption, single scattering albedo, and aerosol hygroscopic response.

Aerosol optical property measurements associated with U.S. Independence Day show a ~4-hour episode with peak light extinction at ~00:35 on 5 July 2016 with minor effects before and after this period. The temporal trends were consistent though later than those found at sites examined across the U.S. [*Seidel and Birnbaum*, 2015], who observed peak impacts at 9-10 pm on July 4$^{th}$ and decreasing to background by noon on July 5$^{th}$. Combined evidence from the timing of the event (several hours after municipal fireworks displays) and meteorology indicates influence of a fireworks display upwind and 40km to the west-southwest at Jemez Springs, NM. From meteorology, consistent westerly winds measured at the Los Alamos airport combined with air-

mass back-trajectory analysis performed here with the NOAA HYSPLIT model shows passage over Jemez Springs, NM. .

Throughout the event, little variability was observed in the intensive aerosol properties of single scattering albedo and Ångström exponent for light scattering, indicating a well-mixed firework smoke plume. Contrastingly, the hygroscopic response, *f*(RH) dropped to a minimum around 1 at the peak of the event indicating a nearly hydrophobic aerosol. Though we lack chemical composition measurements, the aerosol was not strongly soot-dominated as ω increased slightly during the event to $\omega = 0.86 \pm 0.03$ and the BC mass concentration remained low (BC < 0.36 $\mu g/m^3$). We suspect carbonaceous aerosol, and more specifically, organic carbon species contributed substantially to the low hygroscopicity [*Carrico et al.*, 2005] and relatively high value of ω. Past chemical speciation studies of fireworks aerosols have shown a dominance of carbonaceous material and in particular organic carbon, and we suspect this as the case due to modest increases in black carbon and a low hygroscopicity that argues against inorganic salts that would drive larger hygroscopicity.

Our ambient measurements should not be considered universally representative for fireworks smoke as underscored by the strong difference in hygroscopic properties between the sparklers and ambient fireworks smoke we attributed to aerial fireworks. We followed the ambient measurements with lab testing of two sparkler varieties that showed a very strong hygroscopic response which we linked to the colorant compounds and lack of black powder explosives in sparklers. Clearly the composition of the fireworks is key to the hygroscopicity of the smoke, and this is an area for further exploration. Several parallels are found in common between fireworks and biomass smoke: tracers of potassium and chloride, the generally low hygroscopic response of the carbonaceous fraction of each, and the importance of organic carbon compounds.

It is worth reiterating here that most fireworks (approximately two thirds) by dollar amount are associated with private sales to individuals and thus air quality impacts, particularly near ground level, are not limited to professional displays. It is indeterminate which would dominate air quality impacts and likely varies with regional population density and usage. Overall, due to the short time-frame of impacts, no specific regulatory actions are recommended regarding fireworks

446 impacts. However, the weak hygroscopicity and submicron size of the particles would result in a
447 longer atmospheric lifetime than the background aerosol. Exposures can be high and sensitive
448 individuals are advised to remain indoors, or view from upwind or crosswinds directions. The
449 results provide useful data for freshly emitted combustion aerosols that can be used as model
450 inputs for fireworks smoke aerosol microphysical properties.
451

452 ## 5 ACKNOWLEDGMENTS

453 Data from this study is available by emailing the corresponding author (kip.carrico@nmt.edu).
454 This work was supported in part by the U.S. Department of Energy, Office of Science, Office of
455 Workforce Development for Teachers and Scientists (WDTS) under the Visiting Faculty
456 Program (VFP). This work was supported primarily by the U.S. Department of Energy's
457 Atmospheric System Research, an Office of Science, Office of Biological and Environmental
458 Research program under grant F265 (PI MKD). Los Alamos National Laboratory is operated for
459 the DOE by Los Alamos National Security under contract DE-AC52-06NA25396. The New
460 Mexico Consortium provided additional support for this work. The authors gratefully
461 acknowledge Dr. Amy Sullivan at Colorado State University for analysis of the two filters for
462 chemical composition of sparkler smoke. The authors also acknowledge the NOAA Air
463 Resources Laboratory (ARL) for the provision of the HYSPLIT transport and dispersion model
464 and/or READY website (http://www.ready.noaa.gov) used in this publication. The assistance of
465 Thom Rahn, Sanna Sevanto, and Petr Chylek (Los Alamos National Laboratory) and Caroline
466 Allen (New Mexico Institute of Mining and Technology) is acknowledged.
467

468 ## 6 KEYWORDS

469 Fireworks smoke, ultrafine particles, fine mode aerosols, carbonaceous aerosols, photoacoustic
470 extinctiometer (PAX), nephelometer, hygroscopicity

# 7 TABLE AND FIGURE CAPTIONS

Table 1. Means and standard deviations of pressure, temperature, relative humidity conditions for ambient sampled conditions

Table 2. Aerosol optical properties for approximate four-hour blocks before, during and after a fireworks smoke event.

Table 3. Comparison of ambient fireworks smoke aerosol and laboratory measurements of sparklers emissions.

Figure 1. Experimental flow diagram showing photoacoustic extinctiometer (870 nm) and *f(*RH) system (450 nm).

Figure 2. Los Alamos, NM map showing location of sampling site, local wind rose at the Los Alamos Airport, and inset of 48-hour air mass back trajectories at 500-m, 750-m and 1000-m agl (background images courtesy of Google Earth).

Figure 3. Comparison of two nephelometer agreement for ambient aerosols sampled at 1-min during background aerosol conditions and RH < 34% in both instruments.

Figure 4. Aerosol optical properties including (a) extensive parameters of particulate light scattering and absorption coefficients ($\sigma_{sp}$ and $\sigma_{ap}$) and (b) intensive parameters including light scattering wavelength dependence (Ångström exponent, Å), hygroscopic response in light scattering (*f*(RH=85%)), and ratio of aerosol light scattering to extinction (single scattering albedo, ω). Measurements occurred during a fireworks smoke-influenced period at Los Alamos National Lab on 4 July 2016. Periods of largest impacts from smoke showed a nearly hydrophobic aerosol with *f*(RH=85%) ~1.

Figure 5. Relationship between light scattering from the dry reference nephelometer and photoacoustic extinctiometer

Figure 6. κ-neph predicted from 2-component mixture of background aerosol (κ-neph = 0.12) and fireworks smoke aerosol (κ-neph = 0.003) compared to measured values.

Figure 7. Chemical composition of the smoke generated from burning two types of sparklers (a) "Colored Sparker" manufactured in China and (b) "Gold Sparkler manufactured in Thailand.

# 8 TABLES & FIGURES

**Table 1. Means and standard deviations of pressure, temperature, relative humidity conditions for ambient sampled conditions. The sampling site is located at 2149m ASL.**

| Pressure (mbar) | Temperature (K) | Low RH Nephelometer (%) | High RH Nephelometer (%) |
|---|---|---|---|
| 751.3 ± 0.7 | 298.2 ± 0.9 | 18.9 ± 2.4 | 85.4 ± 0.6 |

**Table 2. Aerosol optical properties for approximate four-hour blocks before, during and after a fireworks smoke event.**

| | $\sigma_{sp}$ (870 nm) | | $\sigma_{ap}$ (870 nm) | | $\sigma_{ep}$ (870 nm) | | ω (870 nm) | | BC (μg/m$^3$) | | Å (450/870 nm) | | $\sigma_{sp}$ (450 nm) | | *f(RH = 85%)* | | κ-*neph* | |
|---|---|---|---|---|---|---|---|---|---|---|---|---|---|---|---|---|---|---|
| | mean | stdev | mean | stdev | mean | stdev | mean | stdev | mean | stdev | mean | stdev | mean | stdev | mean | stdev | mean | stdev |
| Before | 2.4 | 0.8 | 0.49 | 0.28 | 2.9 | 0.9 | 0.83 | 0.11 | 0.10 | 0.06 | 2.07 | 0.44 | 8.8 | 0.4 | 1.62 | 0.06 | 0.104 | 0.013 |
| Event | 11.5 | 7.3 | 1.71 | 0.96 | 13.3 | 8.2 | 0.86 | 0.03 | 0.36 | 0.20 | 2.23 | 0.28 | 49.0 | 29.7 | 1.16 | 0.10 | 0.027 | 0.017 |
| After | 4.0 | 1.1 | 0.77 | 0.21 | 4.7 | 1.2 | 0.83 | 0.04 | 0.16 | 0.04 | 2.27 | 0.35 | 17.3 | 3.5 | 1.38 | 0.08 | 0.067 | 0.014 |

**Table 3. Comparison of ambient fireworks smoke aerosol and laboratory measurements of sparklers emissions.**

| Source | *f*(RH=85%) | κ-neph | ω (870nm) | Ångström |
|---|---|---|---|---|
| Ambient fireworks smoke aerosol | 1.16 ± 0.10 | 0.027± 0.017 | 0.86 ± 0.03 | 2.23 ± 0.28 |
| "Colored sparkler" (China) | 3.69 ± 0.37 | 0.30 ± 0.04 | 1.00 ± 0.02 | 1.73 ± 0.24 |
| "Gold sparkler" (Thailand) | 2.61 ± 0.04 | 0.19 ± 0.01 | 0.93 ± 0.02 | 1.96 ± 0.12 |

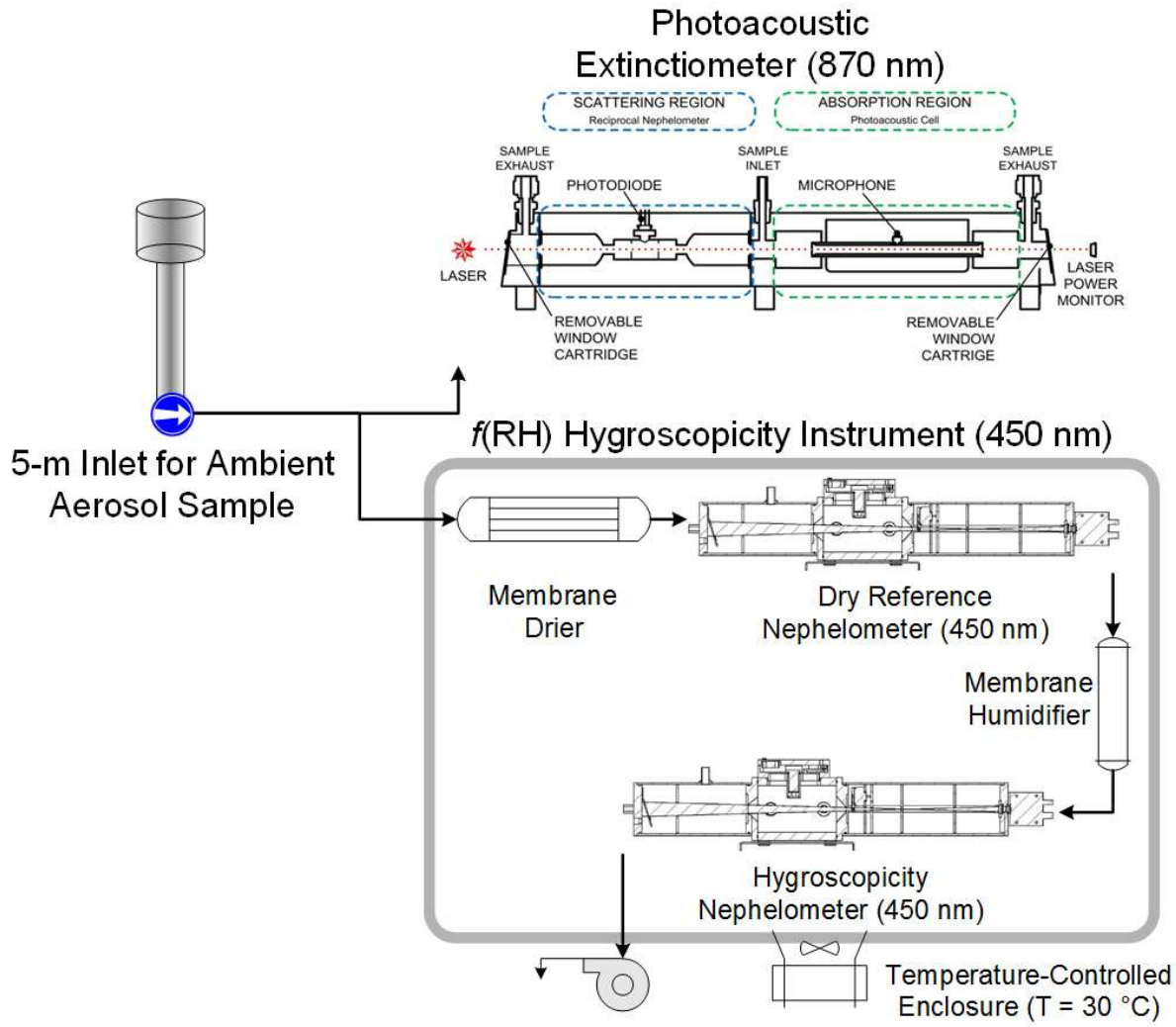


**Figure 1. Experimental flow diagram showing photoacoustic extinctiometer (870 nm) and *f*(RH) system (450 nm).**

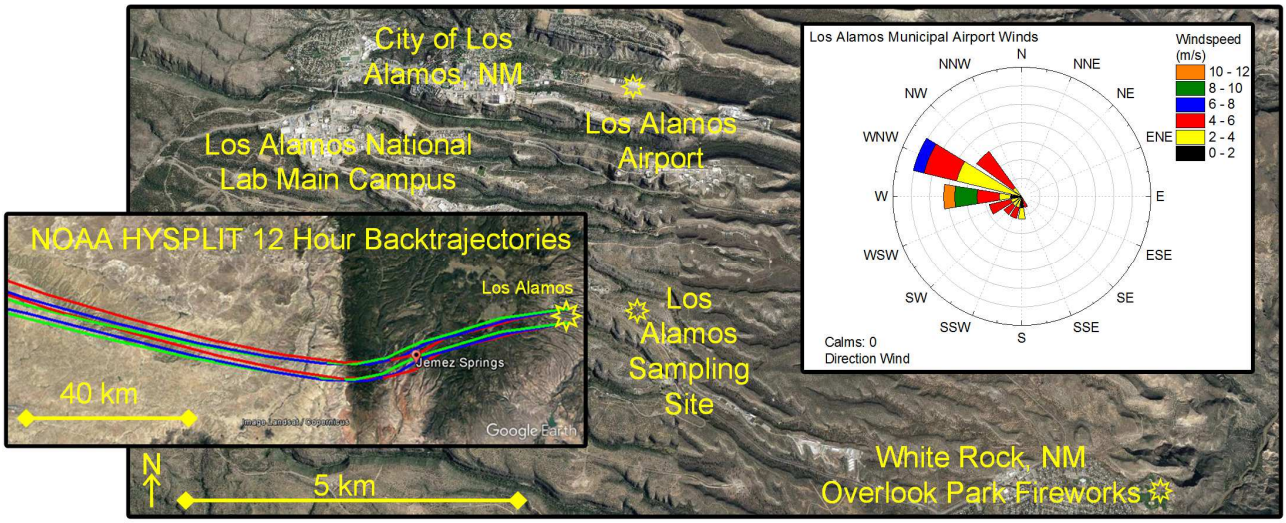


**Figure 2. Los Alamos, NM map showing location of sampling site, local wind rose at the Los Alamos Airport, and inset of 48-hour air mass back trajectories at 500-m, 750-m and 1000-m agl (background images courtesy of Google Earth).**

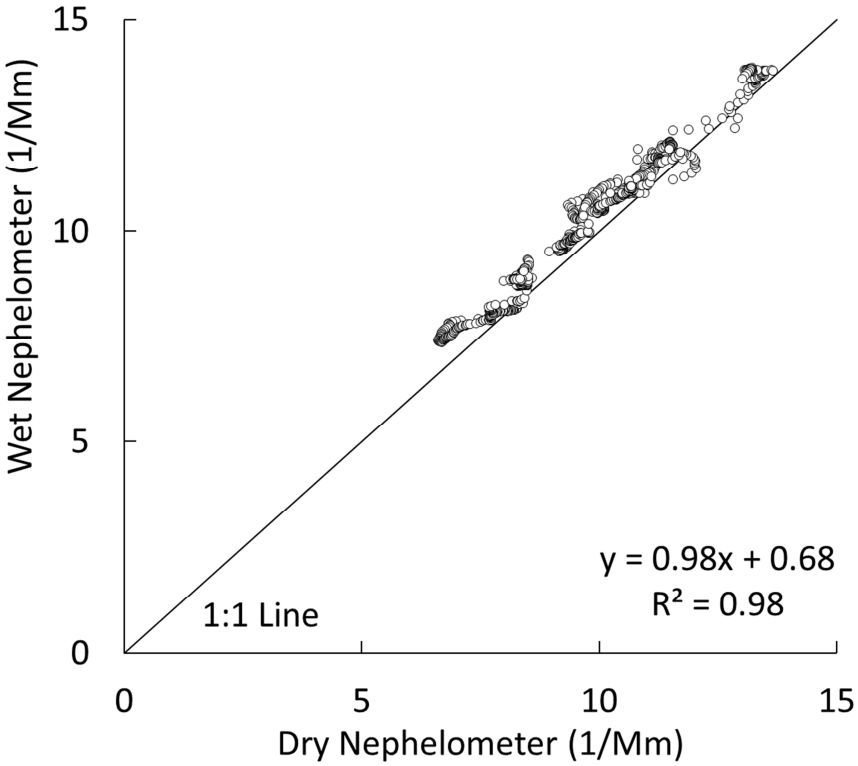


**Figure 3. Comparison of two nephelometer agreement for ambient aerosols sampled at 1-min during background aerosol conditions and RH < 34% in both instruments.**

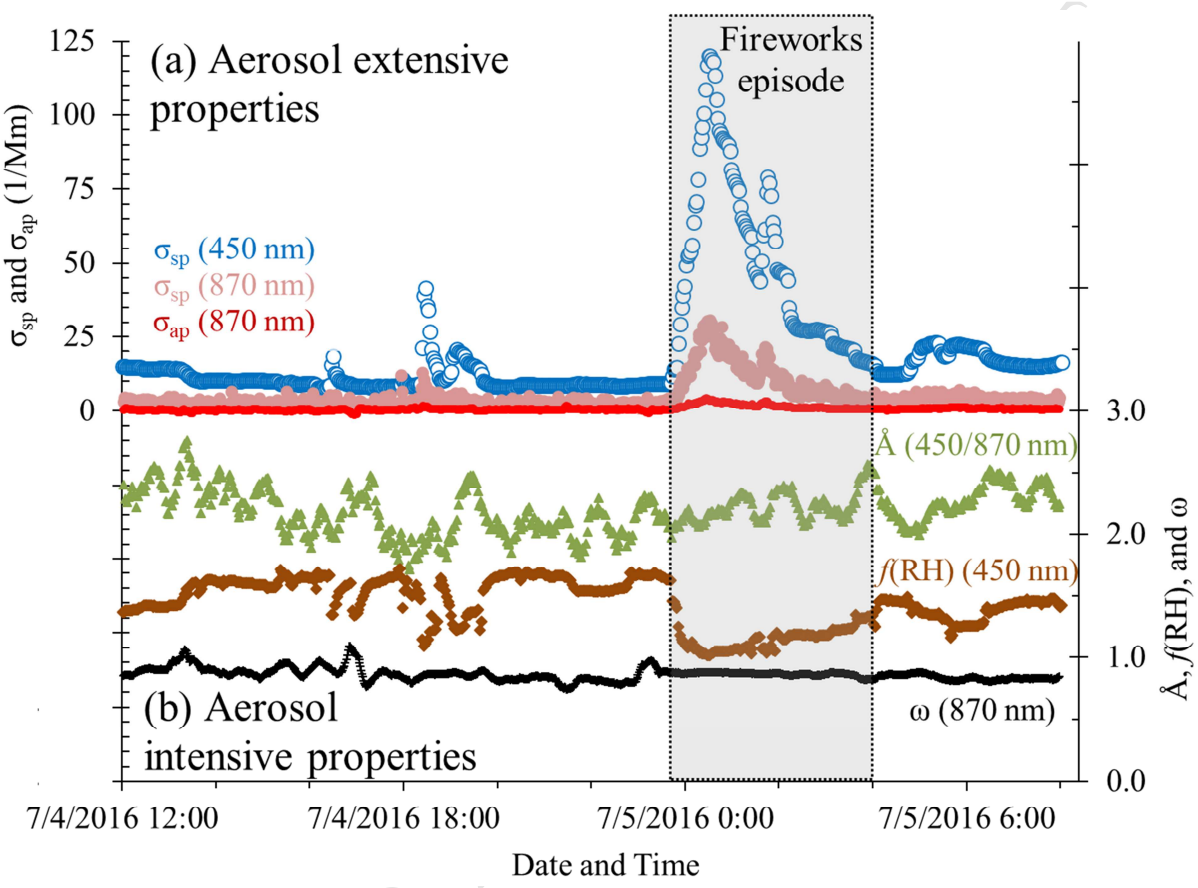


**Figure 4. Aerosol optical properties including (a) extensive parameters of particulate light scattering and absorption coefficients ($\sigma_{sp}$ and $\sigma_{ap}$) and (b) intensive parameters including light scattering wavelength dependence (Ångström exponent, Å), hygroscopic response in light scattering (*f*(RH=85%)), and ratio of aerosol light scattering to extinction (single scattering albedo, ω). Measurements occurred during a fireworks smoke-influenced period at Los Alamos National Lab on 4 July 2016. Periods of largest impacts from smoke showed a nearly hydrophobic aerosol with *f*(RH=85%) ~1.**

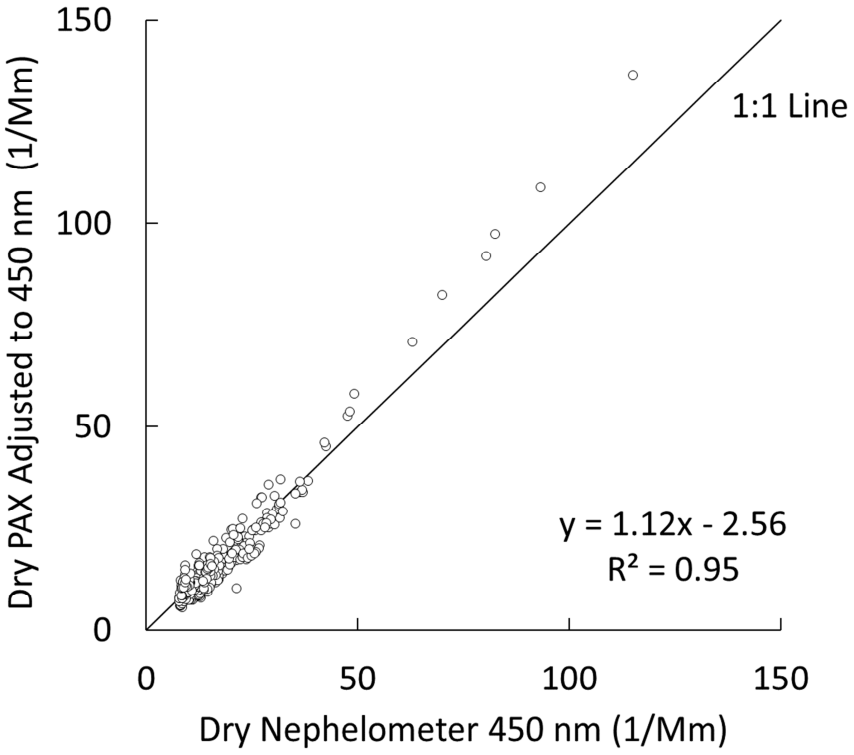


**Figure 5. Relationship between light scattering from the dry reference nephelometer and photoacoustic extinctiometer adjusted to 450 nm with the average Ångström exponent.**

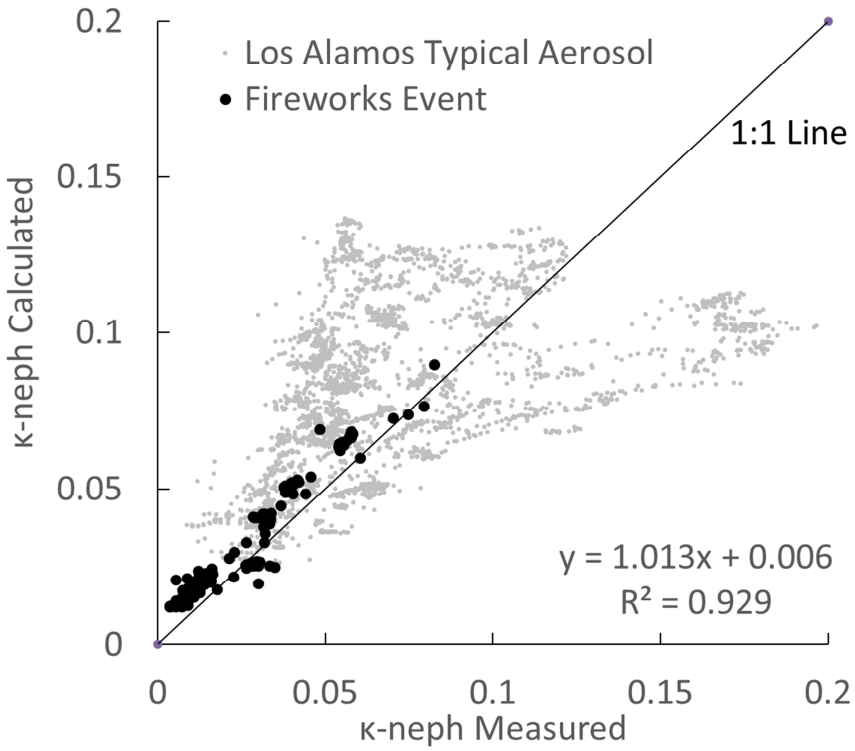


**Figure 6. κ-neph predicted from 2-component mixture of background aerosol (κ-neph = 0.12) and fireworks smoke aerosol (κ-neph = 0.003) compared to measured values.**

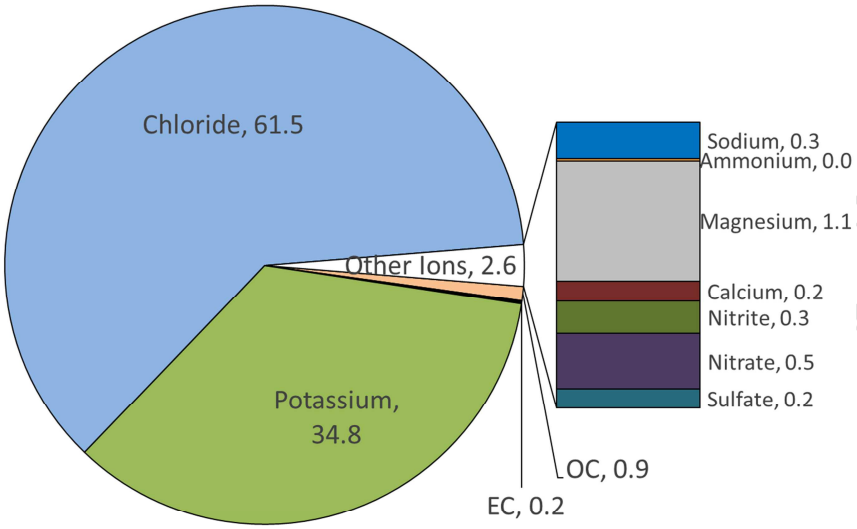


(a) Colored Sparkler (China)

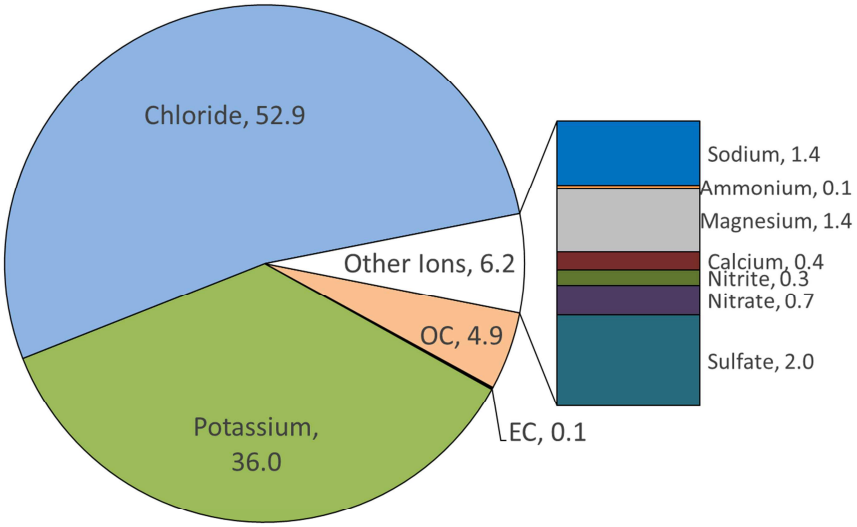


(b) Gold Sparkler (Thailand)

**Figure 7. Chemical composition of the smoke generated from burning two types of sparklers (a) "Colored Sparker" manufactured in China and (b) "Gold Sparkler manufactured in Thailand.**

# 9 REFERENCES

Arnott, W. P., H. Moosmuller, C. F. Rogers, T. F. Jin, and R. Bruch (1999), Photoacoustic spectrometer for measuring light absorption by aerosol: instrument description, *Atmospheric Environment*, *33*(17), 2845-2852.

Arnott, W. P., H. Moosmuller, and J. W. Walker (2000), Nitrogen dioxide and kerosene-flame soot calibration of photoacoustic instruments for measurement of light absorption by aerosols, *Review of Scientific Instruments*, *71*(12), 4545-4552, doi:10.1063/1.1322585.

Attri, A., U. Kumar, and V. Jain (2001), Microclimate - Formation of ozone by fireworks, *Nature*, *411*(6841), 1015-1015, doi:10.1038/35082634.

Betha, R., and R. Balasubramanian (2014), PM2.5 Emissions from Hand-Held Sparklers: Chemical Characterization and Health Risk Assessment, *Aerosol and Air Quality Research*, *14*(5), 1477-1486, doi:10.4209/aaqr.2013.07.0255.

Bond, T. C., et al. (2013), Bounding the role of black carbon in the climate system: A scientific assessment, *Journal of Geophysical Research-Atmospheres*, *118*(11), 5380-5552, doi:10.1002/jgrd.50171.

Brock, C., et al. (2016), Aerosol optical properties in the southeastern United States in summer - Part 1: Hygroscopic growth, *Atmospheric Chemistry and Physics*, *16*(8), 4987-5007, doi:10.5194/acp-16-4987-2016.

Carrico, C., S. Kreidenweis, W. Malm, D. Day, T. Lee, J. Carrillo, G. McMeeking, and J. Collett (2005), Hygroscopic growth behavior of a carbon-dominated aerosol in Yosemite National Park, *Atmospheric Environment*, *39*(8), 1393-1404, doi:10.1016/j.atmosenv.2004.11.029.

Carrico, C., P. Kus, M. Rood, P. Quinn, and T. Bates (2003), Mixtures of pollution, dust, sea salt, and volcanic aerosol during ACE-Asia: Radiative properties as a function of relative humidity, *Journal of Geophysical Research-Atmospheres*, *108*(D23), doi:10.1029/2003JD003405.

Carrico, C., M. Petters, S. Kreidenweis, A. Sullivan, G. McMeeking, E. Levin, G. Engling, W. Malm, and J. Collett (2010), Water uptake and chemical composition of fresh aerosols generated in open burning of biomass, *Atmospheric Chemistry and Physics*, *10*(11), 5165-5178, doi:10.5194/acp-10-5165-2010.

Carrico, C., A. Prenni, S. Kreidenweis, E. Levin, C. McCluskey, P. DeMott, G. McMeeking, S. Nakao, C. Stockwell, and R. Yokelson (2016a), Rapidly evolving ultrafine and fine mode biomass smoke physical properties: Comparing laboratory and field results, *Journal of Geophysical Research-Atmospheres*, *121*(10), 5750-5768, doi:10.1002/2015JD024389.

Carrico, C. M., S. Bixler, C. Allen, M. K. Dubey, A. C. Aiken, T. Rahn, L. Torres, and H. Parker (2016b), Water Uptake and Optical Properties of Biomass Smoke from Southwestern US Fuels: Predicting Properties and Their Variability, in *American Geophysical Union*, edited, San Francisco.

Chen, Y., et al. (2016), Evaluation of impact factors on PM2.5 based on long-term chemical components analyses in the megacity Beijing, China, *Chemosphere*, *155*, 234-242, doi:10.1016/j.chemosphere.2016.04.052.

Devara, P., K. Vijayakumar, P. Safai, M. Raju, and P. Rao (2015), Celebration-induced air quality over a tropical urban station, Pune, India, *Atmospheric Pollution Research*, *6*(3), 511-520, doi:10.5094/APR.2015.057.

Drewnick, F., S. Hings, J. Curtius, G. Eerdekens, and J. Williams (2006), Measurement of fine particulate and gas-phase species during the New Year's fireworks 2005 in Mainz, Germany, *Atmospheric Environment*, *40*(23), 4316-4327, doi:10.1016/j.atmosenv.2006.03.040.

Godri, K., D. Green, G. Fuller, M. Dall'Osto, D. Beddows, F. Kelly, R. Harrison, and I. Mudway (2010), Particulate Oxidative Burden Associated with Firework Activity, *Environmental Science & Technology*, *44*(21), 8295-8301, doi:10.1021/es1016284.

Jiang, Q., Y. Sun, Z. Wang, and Y. Yin (2015), Aerosol composition and sources during the Chinese Spring Festival: fireworks, secondary aerosol, and holiday effects, *Atmospheric Chemistry and Physics*, *15*(11), 6023-6034, doi:10.5194/acp-15-6023-2015.

Kong, S., L. Li, X. Li, Y. Yin, K. Chen, D. Liu, L. Yuan, Y. Zhang, Y. Shan, and Y. Ji (2015), The impacts of firework burning at the Chinese Spring Festival on air quality: insights of tracers, source evolution and aging processes, *Atmospheric Chemistry and Physics*, *15*(4), 2167-2184, doi:10.5194/acp-15-2167-2015.

Kumar, M., R. Singh, V. Murari, A. Singh, R. Singh, and T. Banerjee (2016), Fireworks induced particle pollution: A spatio-temporal analysis, *Atmospheric Research*, *180*, 78-91, doi:10.1016/j.atmosres.2016.05.014.

Lang-Yona, M., Y. Rudich, E. Segre, E. Dinar, and A. Abo-Riziq (2009), Complex Refractive Indices of Aerosols Retrieved by Continuous Wave-Cavity Ring Down Aerosol Spectrometer, *Analytical Chemistry*, *81*(5), 1762-1769, doi:10.1021/ac8017789.

Lin, C., K. Huang, H. Chen, J. Tsai, Y. Chiu, J. Lee, and S. Chen (2014), Influences of Beehive Firework Displays on Ambient Fine Particles during the Lantern Festival in the YanShuei Area of Southern Taiwan, *Aerosol and Air Quality Research*, *14*(7), 1998-2009, doi:10.4209/aaqr.2014.09.0201.

Lin, C., L. Yang, and Y. Cheng (2016), Ambient PM2.5, Black Carbon, and Particle Size-Resolved Number Concentrations and the Angstrom Exponent Value of Aerosols during the Firework Display at the Lantern Festival in Southern Taiwan, *Aerosol and Air Quality Research*, *16*(2), 373-387, doi:10.4209/aaqr.2015.09.0569.

Liu, S., et al. (2014), Aerosol single scattering albedo dependence on biomass combustion efficiency: Laboratory and field studies, *Geophysical Research Letters*, *41*(2), 742-748, doi:10.1002/2013GL058392.

Mandal, P., M. Prakash, and J. Bassin (2012), Impact of Diwali celebrations on urban air and noise quality in Delhi City, India, *Environmental Monitoring and Assessment*, *184*(1), 209-215, doi:10.1007/s10661-011-1960-7.

Moreno, T., X. Querol, A. Alastuey, M. Minguillon, J. Pey, S. Rodriguez, J. Miro, C. Felis, and W. Gibbons (2007), Recreational atmospheric pollution episodes: Inhalable metalliferous particles from firework displays, *Atmospheric Environment*, *41*(5), 913-922, doi:10.1016/j.atmosenv.2006.09.019.

Muller, T., M. Laborde, G. Kassell, and A. Wiedensohler (2011), Design and performance of a three-wavelength LED-based total scatter and backscatter integrating nephelometer, *Atmospheric Measurement Techniques*, *4*(6), 1291-1303, doi:10.5194/amt-4-1291-2011.

Nakayama, T., H. Suzuki, S. Kagamitani, Y. Ikeda, A. Uchiyama, and Y. Matsumi (2015), Characterization of a Three Wavelength Photoacoustic Soot Spectrometer (PASS-3) and a Photoacoustic Extinctiometer (PAX), *Journal of the Meteorological Society of Japan*, *93*(2), 285-308, doi:10.2151/jmsj.2015-016.

Nasir, U., and D. Brahmaiah (2015), Impact of fireworks on ambient air quality: a case study, *International Journal of Environmental Science and Technology*, *12*(4), 1379-1386, doi:10.1007/s13762-014-0518-y.

Parkhi, N., et al. (2016), Large inter annual variation in air quality during the annual festival 'Diwali' in an Indian megacity, *Journal of Environmental Sciences*, *43*, 265-272, doi:10.1016/j.jes.2015.08.015.

Pope, C., and D. Dockery (2006), Health effects of fine particulate air pollution: Lines that connect, *Journal of the Air & Waste Management Association*, *56*(6), 709-742.

Raju, M., P. Safai, P. Rao, S. Tiwari, and P. Devara (2014), Impact of anthropogenic activity and cyclonic storm on black carbon during winter at a tropical urban city, Pune, *Natural Hazards*, *71*(1), 881-894, doi:10.1007/s11069-013-0937-y.

Reid, J., T. Eck, S. Christopher, R. Koppmann, O. Dubovik, D. Eleuterio, B. Holben, E. Reid, and J. Zhang (2005a), A review of biomass burning emissions part III: intensive optical properties of biomass burning particles, *Atmospheric Chemistry and Physics*, *5*, 827-849.

Reid, J., R. Koppmann, T. Eck, and D. Eleuterio (2005b), A review of biomass burning emissions part II: intensive physical properties of biomass burning particles, *Atmospheric Chemistry and Physics*, *5*, 799-825.

Rolph, G. D. (2017), Real-time Environmental Applications and Display sYstem (READY), (http://www.ready.noaa.gov). NOAA Air Resources Laboratory, College Park, MD, edited.

Russell, M. S. (2000), *The Chemistry of Fireworks*, Royal Society of Chemistry, Cambridge, UK.

Saleh, R., et al. (2014), Brownness of organics in aerosols from biomass burning linked to their black carbon content, *Nature Geoscience*, *7*(9), 647-650, doi:10.1038/ngeo2220.

Seidel, D., and A. Birnbaum (2015), Effects of Independence Day fireworks on atmospheric concentrations of fine particulate matter in the United States, *Atmospheric Environment*, *115*, 192-198, doi:10.1016/j.atmosenv.2015.05.065.

Stein, A., R. Draxler, G. Rolph, B. Stunder, M. Cohen, and F. Ngan (2015), NOAA'S HYSPLIT Atmospheric Transport and Dispersion Modeling System, *Bulletin of the American Meteorological Society*, *96*(12), 2059-2077, doi:10.1175/BAMS-D-14-00110.1.

Tsai, H., L. Chien, C. Yuan, Y. Lin, Y. Jen, and I. Ie (2012), Influences of fireworks on chemical characteristics of atmospheric fine and coarse particles during Taiwan's Lantern Festival, *Atmospheric Environment*, *62*, 256-264, doi:10.1016/j.atmosenv.2012.08.012.

Vakkari, V., et al. (2014), Rapid changes in biomass burning aerosols by atmospheric oxidation, *Geophysical Research Letters*, *41*(7), 2644-2651, doi:10.1002/2014gl059396.

Wang, Y., P. Hopke, and O. Rattigan (2012), A new indicator of fireworks emissions in Rochester, New York, *Environmental Monitoring and Assessment*, *184*(12), 7293-7297, doi:10.1007/s10661-011-2497-5.

Yao, L., et al. (2015), Levels, indoor-outdoor relationships and exposure risks of airborne particle-associated perchlorate and chlorate in two urban areas in Eastern Asia, *Chemosphere*, *135*, 31-37, doi:10.1016/j.chemosphere.2015.03.026.

Yerramsetti, V., A. Sharma, N. Navlur, V. Rapolu, N. Dhulipala, and P. Sinha (2013), The impact assessment of Diwali fireworks emissions on the air quality of a tropical urban site, Hyderabad, India, during three consecutive years, *Environmental Monitoring and Assessment*, *185*(9), 7309-7325, doi:10.1007/s10661-013-3102-x.

# Low Hygroscopicity of Ambient Fresh Carbonaceous Aerosols from Pyrotechnics Smoke

**Christian M. Carrico*, Samantha L. Bixler** New Mexico Institute of Mining and Technology, Socorro, NM 87801

**Manvendra K. Dubey, Allison C. Aiken** Los Alamos National Laboratory, Los Alamos, NM 87545

## HIGHLIGHTS

1. Pyrotechnics (fireworks) have substantial though episodic impacts on ambient aerosol properties.
2. In a well-mixed < 3 hr old fireworks plume, dry light scattering (450 nm) reached 120 $Mm^{-1}$ with nearly constant ω (780nm) = 0.86 and Å = 2.2.
3. Ambient fireworks smoke aerosol hygroscopic response was low (*f*(RH=85%) ~ 1), implying lower radiative effects but longer lifetime and potential human exposures.
4. Chemical composition was a key driver as smoke from small sparklers exhibited greater water uptake (due to the contribution of potassium chloride) than from the larger explosive aerial fireworks which were likely dominated by organic and elemental carbon.